Hibi T, Inazawa J, Watanabe M 2002 Damaged epithelia regenerated by bone marrow-derived cells in the human gastrointestinal tract. Nat Med 8:1011-7

7. **Lee VM, Stoffel M** 2003 Bone marrow: an extra-pancreatic hideout for the elusive pancreatic stem cell? J Clin Invest 111:799-801

8. **Lechner A, Habener JF** 2003 Bone marrow stem cells find a path to the pancreas. Nat Biotechnol 21:755-6

9. **Tessem JS, DeGregori J** 2004 Roles for bone-marrow-derived cells in beta-cell maintenance. Trends Mol Med 10:558-64

10. **Ianus A, Holz GG, Theise ND, Hussain MA** 2003 In vivo derivation of glucose-competent pancreatic endocrine cells from bone marrow without evidence of cell fusion. J Clin Invest 111:843-50

11. **Choi JB, Uchino H, Azuma K, Iwashita N, Tanaka Y, Mochizuki H, Migita M, Shimada T, Kawamori R, Watada H** 2003 Little evidence of transdifferentiation of bone marrow-derived cells into pancreatic beta cells. Diabetologia 46:1366-74

12. **Lechner A, Yang YG, Blacken RA, Wang L, Nolan AL, Habener JF** 2004 No evidence for significant transdifferentiation of bone marrow into pancreatic beta-cells in vivo. Diabetes 53:616-23

13. **Taneera J, Rosengren A, Renstrom E, Nygren JM, Serup P, Rorsman P, Jacobsen SE** 2006 Failure of Transplanted Bone Marrow Cells to Adopt a

Pancreatic {beta}-Cell Fate. Diabetes 55:290-6

14. **Hess D, Li L, Martin M, Sakano S, Hill D, Strutt B, Thyssen S, Gray DA, Bhatia M** 2003 Bone marrow-derived stem cells initiate pancreatic regeneration. Nat Biotechnol 21:763-70

15. **Banerjee M, Kumar A, Bhonde RR** 2005 Reversal of experimental diabetes by multiple bone marrow transplantation. Biochem Biophys Res Commun 328:318-25

16. **Izumida Y, Aoki T, Yasuda D, Koizumi T, Suganuma C, Saito K, Murai N, Shimizu Y, Hayashi K, Odaira M, Kusano T, Kushima M, Kusano M** 2005 Hepatocyte growth factor is constitutively produced by donor-derived bone marrow cells and promotes regeneration of pancreatic beta-cells. Biochem Biophys Res Commun 333:273-282

17. **Li FX, Zhu JW, Tessem JS, Beilke J, Varella-Garcia M, Jensen J, Hogan CJ, DeGregori J** 2003 The development of diabetes in E2f1/E2f2 mutant mice reveals important roles for bone marrow-derived cells in preventing islet cell loss. Proc Natl Acad Sci U S A 100:12935-40

18. **Than S, Ishida H, Inaba M, Fukuba Y, Seino Y, Adachi M, Imura H, Ikehara S** 1992 Bone marrow transplantation as a strategy for treatment of non-insulin-dependent diabetes mellitus in KK-Ay mice. J Exp Med 176:1233-8

19. **Mathews V, Hanson PT, Ford E, Fujita J, Polonsky KS, Graubert TA** 2004

Recruitment of bone marrow-derived endothelial cells to sites of pancreatic beta-cell injury. Diabetes 53:91-8

20. **Aicher A, Heeschen C, Mildner-Rihm C, Urbich C, Ihling C, Technau-Ihling K, Zeiher AM, Dimmeler S** 2003 Essential role of endothelial nitric oxide synthase for mobilization of stem and progenitor cells. Nat Med 9:1370-6

21. **Okabe M, Ikawa M, Kominami K, Nakanishi T, Nishimune Y** 1997 'Green mice' as a source of ubiquitous green cells. FEBS Lett 407:313-9

22. **Wang Z, Dohle C, Friemann J, Green BS, Gleichmann H** 1993 Prevention of high- and low-dose STZ-induced diabetes with D-glucose and 5-thio-D-glucose. Diabetes 42:420-8

23. **Ishihara H, Takeda S, Tamura A, Takahashi R, Yamaguchi S, Takei D, Yamada T, Inoue H, Soga H, Katagiri H, Tanizawa Y, Oka Y** 2004 Disruption of the WFS1 gene in mice causes progressive beta-cell loss and impaired stimulus-secretion coupling in insulin secretion. Hum Mol Genet 13:1159-70

24. **Ramiya VK, Maraist M, Arfors KE, Schatz DA, Peck AB, Cornelius JG** 2000 Reversal of insulin-dependent diabetes using islets generated in vitro from pancreatic stem cells. Nat Med 6:278-82

25. **Bonner-Weir S, Taneja M, Weir GC, Tatarkiewicz K, Song KH, Sharma A, O'Neil JJ** 2000 In vitro cultivation of human islets from expanded ductal tissue. Proc Natl Acad Sci U S A 97:7999-8004

26. **Gao R, Ustinov J, Pulkkinen MA, Lundin K, Korsgren O, Otonkoski T** 2003 Characterization of endocrine progenitor cells and critical factors for their differentiation in human adult pancreatic cell culture. Diabetes 52:2007-15

27. **Ema H, Suda T, Nakauchi H, Nakamura Y, Iwama A, Imagawa S, Akutsu M, Kano Y, Kato S, Yabe M, et al.** 1991 Multipotent and committed CD34+ cells in bone marrow transplantation. Jpn J Cancer Res 82:547-52

28. **Tropepe V, Coles BL, Chiasson BJ, Horsford DJ, Elia AJ, McInnes RR, van der Kooy D** 2000 Retinal stem cells in the adult mammalian eye. Science 287:2032-6

29. **Okano H** 2002 Neural stem cells: progression of basic research and perspective for clinical application. Keio J Med 51:115-28

30. **Trucco M** 2005 Regeneration of the pancreatic beta cell. J Clin Invest 115:5-12

31. **Blyszczuk P, Wobus AM** 2004 Stem cells and pancreatic differentiation in vitro. J Biotechnol 113:3-13

32. **Dor Y, Brown J, Martinez OI, Melton DA** 2004 Adult pancreatic beta-cells are formed by self-duplication rather than stem-cell differentiation. Nature 429:41-6

33. **Georgia S, Bhushan A** 2004 Beta cell replication is the primary mechanism for maintaining postnatal beta cell mass. J Clin Invest 114:963-8

34. **Heissig B, Hattori K, Dias S, Friedrich M, Ferris B, Hackett NR, Crystal RG, Besmer P, Lyden D, Moore MA, Werb Z, Rafii S** 2002 Recruitment of stem

and progenitor cells from the bone marrow niche requires MMP-9 mediated release of kit-ligand. Cell 109:625-37

35. **Menger MD, Vajkoczy P, Leiderer R, Jager S, Messmer K** 1992 Influence of experimental hyperglycemia on microvascular blood perfusion of pancreatic islet isografts. J Clin Invest 90:1361-9

36. **Lammert E, Cleaver O, Melton D** 2001 Induction of pancreatic differentiation by signals from blood vessels. Science 294:564-7

37. **Nikolova G, Jabs N, Konstantinova I, Domogatskaya A, Tryggvason K, Sorokin L, Fassler R, Gu G, Gerber HP, Ferrara N, Melton DA, Lammert E** 2006 The vascular basement membrane: a niche for insulin gene expression and Beta cell proliferation. Dev Cell 10:397-405

38. **Otani A, Kinder K, Ewalt K, Otero FJ, Schimmel P, Friedlander M** 2002 Bone marrow-derived stem cells target retinal astrocytes and can promote or inhibit retinal angiogenesis. Nat Med 8:1004-10

39. **Higashi Y, Kimura M, Hara K, Noma K, Jitsuiki D, Nakagawa K, Oshima T, Chayama K, Sueda T, Goto C, Matsubara H, Murohara T, Yoshizumi M** 2004 Autologous bone-marrow mononuclear cell implantation improves endothelium-dependent vasodilation in patients with limb ischemia. Circulation 109:1215-8

Figure Legends

Figure 1. Bone marrow transplantation (BMT) in streptozotocin (STZ)-treated mice.

A. Experimental protocol.

B. Bone marrow chimerism. *Left upper panels*: bright field, *left lower panels*: FITC and *right panels*: representative FACS analyses of bone marrow chimerism from C57BL/6J mice (a), GFP transgenic mice (b), STZ-treated mice receiving lethal irradiation and BMT from GFP transgenic mice and (c) and STZ-treated mice infused with BM cells of GFP transgenic mice, without pre-irradiation (d).

C. Fasting blood glucose of STZ-treated mice with or without BMT. ▲:STZ-treated mice without BMT (hyperglycemic control), ■: STZ-treated mice receiving BMT (lethal irradiation and subsequent BM cell infusion from GFP transgenic mice.), ●: STZ-treated mice infused with BM cells of GFP transgenic mice, without pre-irradiation. ○: mice with neither STZ nor BMT (normoglycemic control). * $p<0.05$ for ■ compared with ▲ group. n=5-6 in each group.

D. Fasting plasma insulin on day 40. Cont: mice with neither STZ nor BMT (normoglycemic control), STZ: STZ-treated mice without BMT (hyperglycemic control), STZ+BMT: STZ-treated mice receiving BMT. * $p<0.05$ for STZ+BMT compared with STZ group. n=5-6 in each group.

Figure 2. Pancreatic islets of STZ-treated mice receiving subsequent BMT.

A. Hematoxylin-Eosin (HE) staining of pancreases on day 35. Pancreases from normoglycemic control mouse (a and e), hyperglycemic control mouse (b and f), STZ-treated mouse simply infused with BM cells without pre-irradiation (c and g) and STZ-treated mouse receiving lethal irradiation and BMT (d and h). a-d: 40 x, and e-h: 100 x magnification.

B. Anti-insulin immunostaining of pancreases. Pancreases from normoglycemic control mouse (a), hyperglycemic control mouse (b) and STZ-treated mouse receiving BMT (c and d). a-c: 40 x, and d: 200 x magnification.

C. Double immunostaining of pancreas with anti-insulin and anti-keratin/cytokeratin antibodies. Green indicates insulin-positive and red keratin/cytokeratin-positive cells, i.e. pancreatic ductal epithelium.

D. Double immunostaining of pancreases with anti-insulin and anti-glucagon antibodies. Pancreases from normoglycemic control mouse (a), hyperglycemic control mouse (b) and STZ-treated mouse receiving BMT (c).

In C and D, to avoid overlapping staining of GFP with FITC, BM cells obtained from wild-type C57BL/6J mice, but not from GFP transgenic mice, were transplanted. Representative histological findings among six independent experiments are presented.

Figure 3. BrdU-positive proliferating cells in pancreases of STZ-treated mice

receiving subsequent BMT.

(A-C) Pancreases from normoglycemic control mouse (A), hyperglycemic control mouse (B) and STZ-treated mice receiving BMT (C) (10 days after BMT). Brown cells are BrdU-positive.

(D) Double immunostaining of pancreases from STZ-treated mice receiving BMT (10 days after BMT) with anti-insulin and anti-BrdU. Brown and red cells are BrdU- and insulin-positive, respectively.

Figure 4. BM-derived cells in pancreases of STZ-treated mice receiving subsequent BMT.

A. BM-derived cells and insulin-positive cells in pancreas of STZ-treated mouse receiving BMT from GFP transgenic mice. Pancreases of STZ-treated mouse receiving subsequent BMT from GFP transgenic mice (35 days after the first STZ). a: insulin-positive cells, b: GFP-positive, i.e. BM-derived cells and c: merged image of a and b.

B. BM-derived cells in pancreases of STZ-treated mice receiving BMT from GFP transgenic mice. Brown cells are GFP-positive, i.e. BM-derived cells, and arrows indicate islets.

C. CD45-positive and BM-derived cells in pancreas of STZ-treated m-ice receiving BMT from GFP transgenic mice. a. Immunostaining with anti-CD45 antibody. Red indicates

CD45-positive cells. b. Green indicates GFP-positive cells. c: merged image of a and b. Yellow indicates GFP and CD45 double positive cells. Arrows indicate islets.

D. CD31 (PECAM-1)-positive and BM-derived cells in pancreases of STZ-treated mice receiving BMT from GFP transgenic mice. a. Immunostaining with anti-CD31 antibody. Red indicates CD31-positive cells. b. Green indicates GFP-positive cells. c: Merged image of a and b.

Figure 5. BMT experiments using *Nos3*$^{+/+}$ and *Nos3*$^{-/-}$ mice.

A. Time courses of peripheral WBC counts in *Nos3*$^{+/+}$ and *Nos3*$^{-/-}$ mice receiving BMT. ■: STZ-treated *Nos3*$^{+/+}$ mice receiving BMT from *Nos3*$^{+/+}$ mice, ▲: STZ-treated *Nos3*$^{-/-}$ mice receiving BMT from *Nos3*$^{-/-}$ mice, and ●: STZ-treated *Nos3*$^{+/+}$ mice receiving BMT from *Nos3*$^{-/-}$ mice. * $p<0.05$ for ▲ compared with ■ group, and # $p<0.05$ for ● compared with ▲ group, respectively. n=5-6 in each group.

B. Fasting blood glucose levels of *Nos3*$^{+/+}$ and *Nos3*$^{-/-}$ receiving BMT. ○: Normoglycemic control *Nos3*$^{+/+}$ mice with neither STZ nor BMT; Δ: STZ-treated *Nos3*$^{+/+}$ mice without BMT (hyperglycemic control), ■: STZ-treated *Nos3*$^{+/+}$ mice receiving BMT from *Nos3*$^{+/+}$ mice, ▲: STZ-treated *Nos3*$^{-/-}$ mice receiving BMT from *Nos3*$^{-/-}$ mice, ●: STZ-treated *Nos3*$^{+/+}$ mice receiving BMT from *Nos3*$^{-/-}$ mice. * $p<0.05$ for ● compared with Δ group, and # $p<0.05$ for ■ compared with ● group, respectively. n=5-6 in each group.

C. Pancreatic insulin contents. STZ: STZ-treated *Nos3*$^{+/+}$ mice without BMT; Cont: *Nos3*$^{+/+}$ or *Nos3*$^{-/-}$ mice with neither STZ nor BMT; STZ+BMT: STZ-treated *Nos3*$^{+/+}$ mice receiving BMT from *Nos3*$^{+/+}$ mice and STZ-treated *Nos3*$^{-/-}$ mice receiving BMT from *Nos3*$^{-/-}$ mice. * $p<0.05$ between STZ-treated *Nos3*$^{+/+}$ mice receiving BMT from *Nos3*$^{+/+}$ mice and STZ-treated *Nos3*$^{-/-}$ mice receiving BMT from *Nos3*$^{-/-}$ mice.

D. Time courses of islet numbers after BMT.

E. Time courses of BrdU-positive cell percentage per islet cells after BMT.

In D and E, the thick line indicates STZ-treated *Nos3*$^{+/+}$ mice receiving BMT from *Nos3*$^{+/+}$ mice and the dotted line STZ-treated *Nos3*$^{-/-}$ mice receiving BMT from *Nos3*$^{-/-}$ mice. * $p<0.05$ between STZ-treated *Nos3*$^{+/+}$ mice receiving BMT from *Nos3*$^{+/+}$ mice and STZ-treated *Nos3*$^{-/-}$ mice receiving BMT from *Nos3*$^{-/-}$ mice at the same time points.

F. Immunostaining of pancreases with anti-insulin and anti-CD45 antibodies. Pancreases from normoglycemic control mice (*Nos3*$^{+/+}$ mouse in a and *Nos3*$^{-/-}$ mouse in f), hyperglycemic control mice (*Nos3*$^{+/+}$ mouse in b and *Nos3*$^{-/-}$ mouse in g), STZ-treated *Nos3*$^{+/+}$ mice receiving BMT from *Nos3*$^{+/+}$ mice (7 days after BMT in c and d, 14 days after BMT in e) and STZ-treated *Nos3*$^{-/-}$ mice receiving BMT from *Nos3*$^{-/-}$ mice (7 days after BMT in h and i, 14 days after BMT in j). Green indicates insulin-positive, red CD45-positive cells. Red arrows indicate CD45-positive cells in and around islets and white arrows pancreatic ducts and blood vessels.

	Days after BMT	Islet numbers	Numbers of BrdU-positive cells	Numbers of cells in islets	Percentage of BrdU-positive cells among islet cells (%)
STZ (-) control	—	94.0±17.3	33.3±4.5	7174±1487	0.51±0.08
STZ+BMT (days after BMT)	0	62.0±11.9	20.6±5.6	4658±1019	0.47±0.11
	3	48.3±2.0	40.7±16.2	2974±278	1.41±0.51
	7	102.7±11.6	194.3±33.4*	6159±528	3.10±0.31*
	10	138.0±22.9*	253.0±107.8*	7989±756*	3.40±1.63
	15	113.7±6.9*	64.7±16.3	5223±539	1.34±0.40
	25	82.0±6.4	37.5±0.4	3953±157	0.95±0.03

* $p<0.05$ vs. day 0 in STZ+BMT group

Table 1. Islet numbers and BrdU-positive cells per pancreatic islet cells of STZ-treated mice receiving subsequent BMT.

To calculate numbers of islets and cells per islet and the percentage of BrdU-positive cells among islet cells, we microscopically examined the whole pancreas in 30 μm sections, and counted the numbers of islets, islet cells and BrdU-positive nuclei in islets.

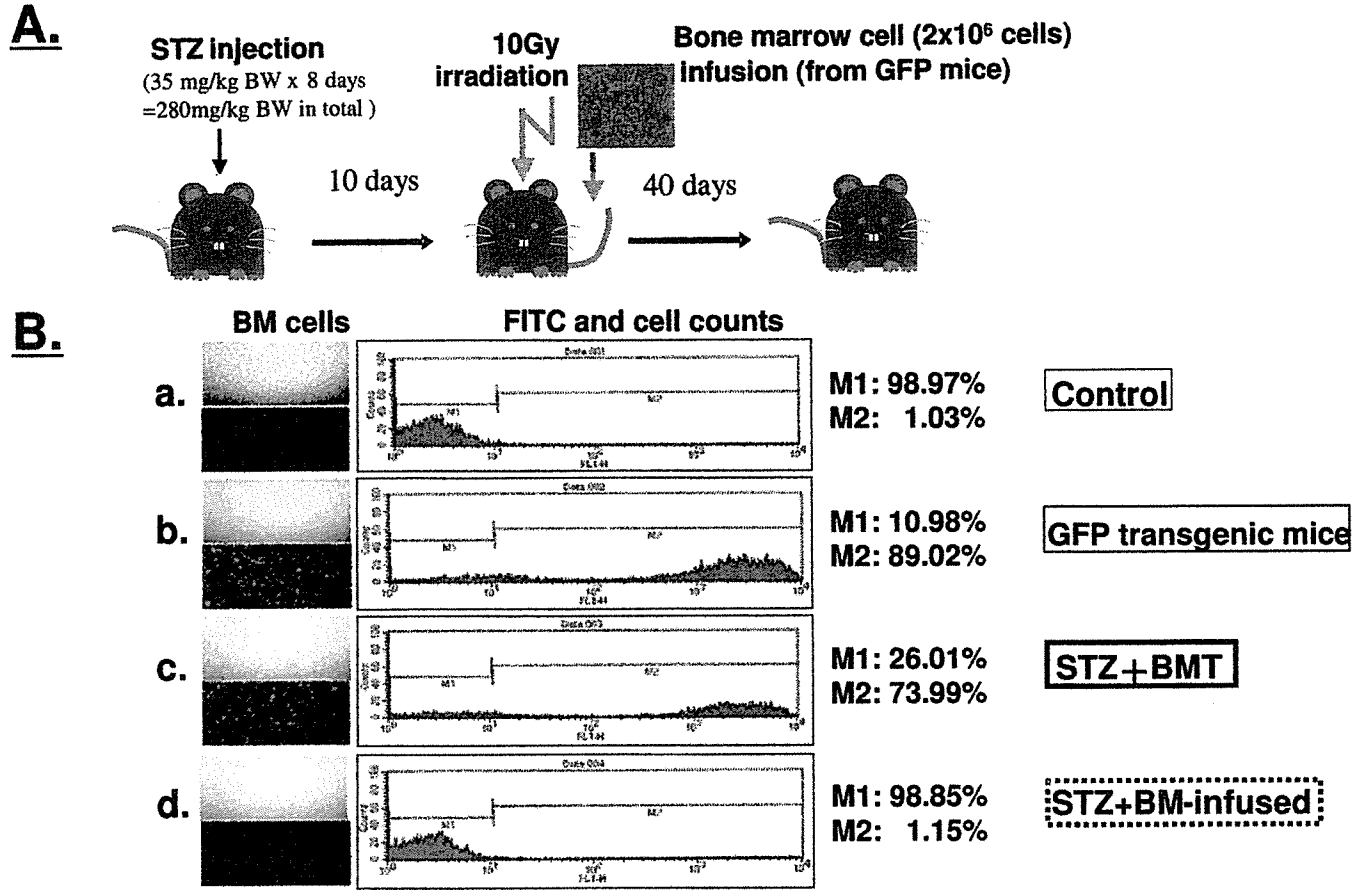
A.
STZ injection
(35 mg/kg BW x 8 days
=280mg/kg BW in total)
10 days
10Gy
irradiation
Bone marrow cell (2x10⁶ cells)
infusion (from GFP mice)
40 days
B.
BM cells
FITC and cell counts
a.
M1: 98.97%
M2: 1.03%
Control
b.
M1: 10.98%
M2: 89.02%
GFP transgenic mice
c.
M1: 26.01%
M2: 73.99%
STZ+BMT
d.
M1: 98.85%
M2: 1.15%
STZ+BM-infused
C.
Fasting blood glucose (mg/dl)
600
500
400
300
200
100
0
1
10
15
20
30
40
50
Days after STZ administration
STZ only
STZ+BM-infused
STZ+BMT
Control
STZ (35 mg/kg BW)
daily for 8 days
10 Gyirradiation
+BMT(in ■ group)
D.
Plasma insulin (ng/ml)
800
700
600
500
400
300
200
100
0
Cont
STZ
STZ
+BMT

Hasegawa, et al. Figure 2

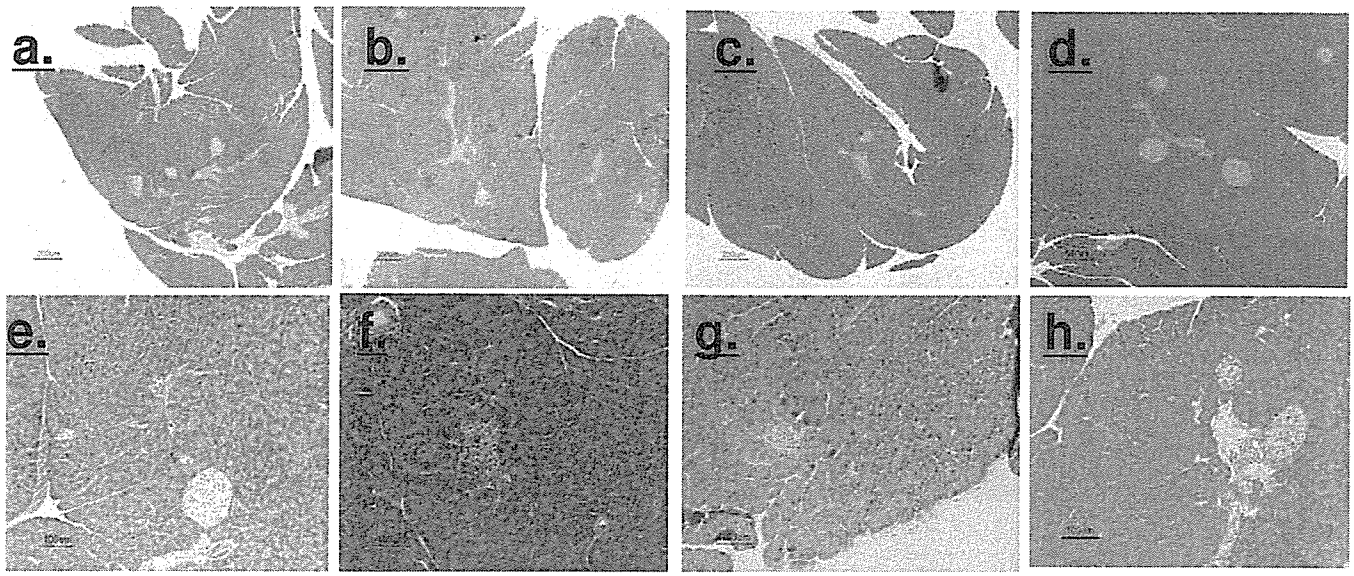

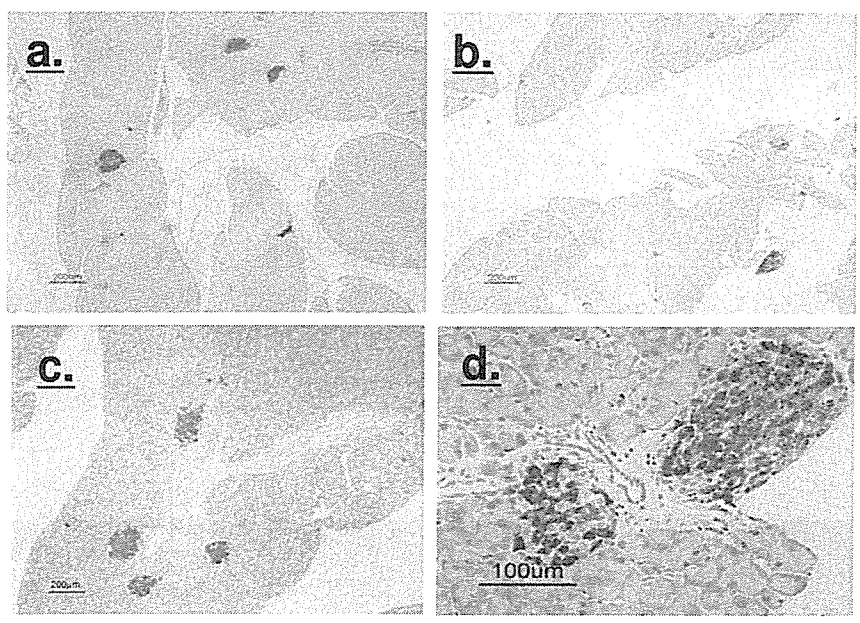

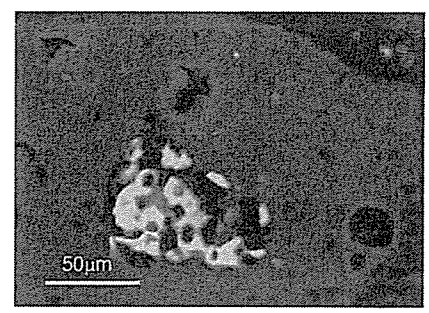

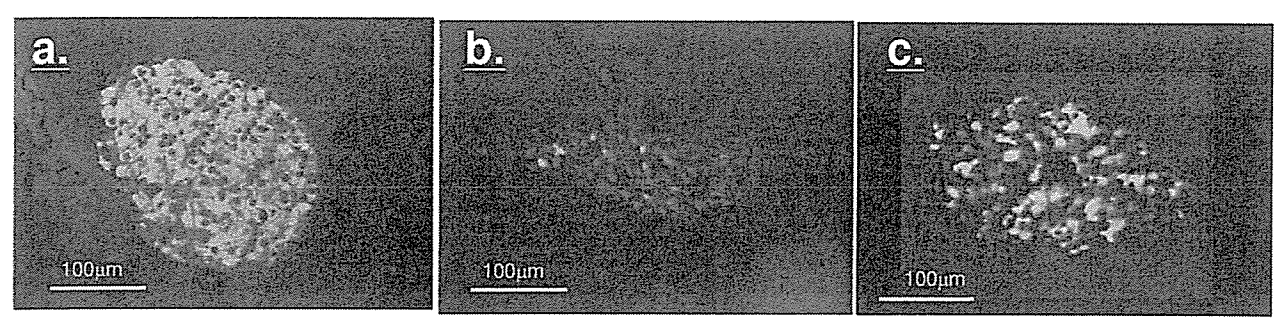

Hasegawa, et al. Figure 3

A.

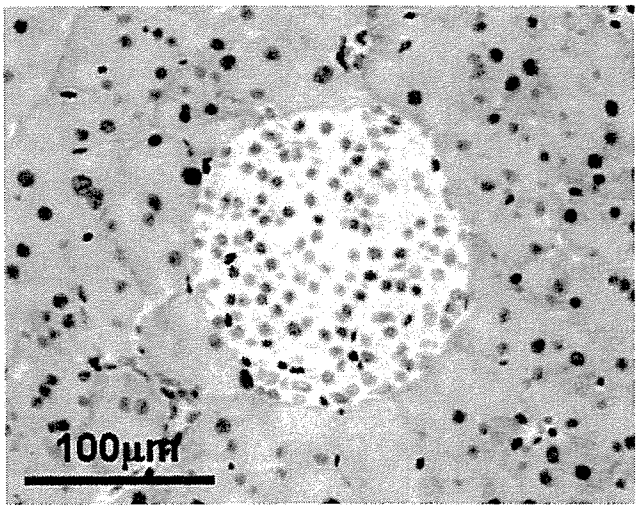

B.

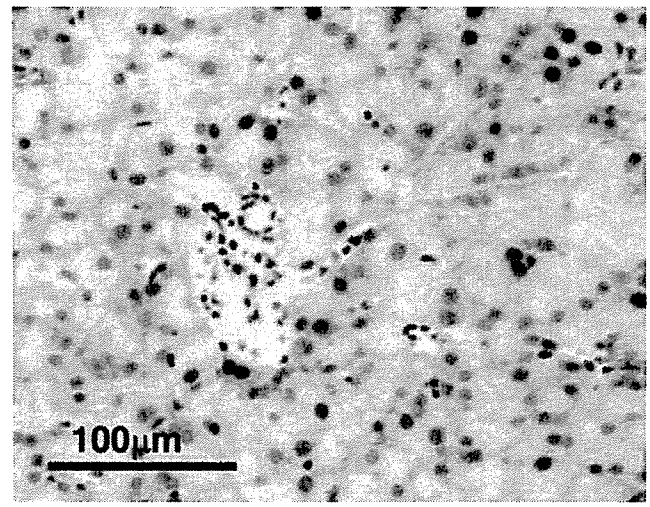

C.

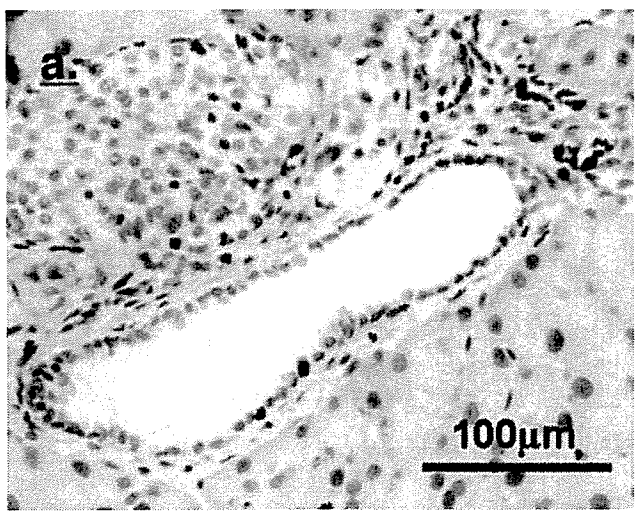

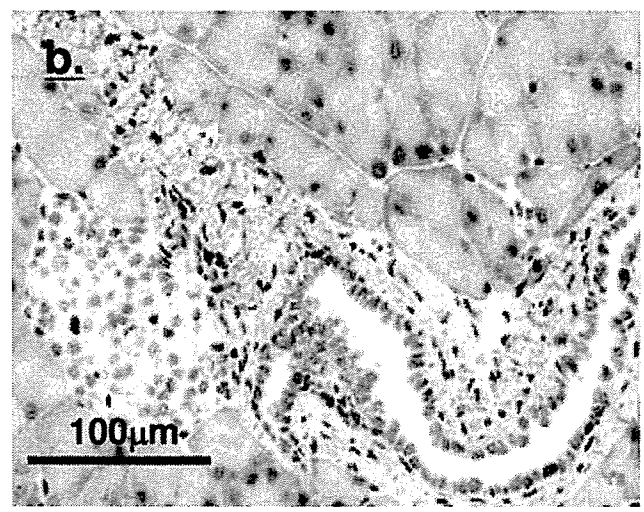

D.

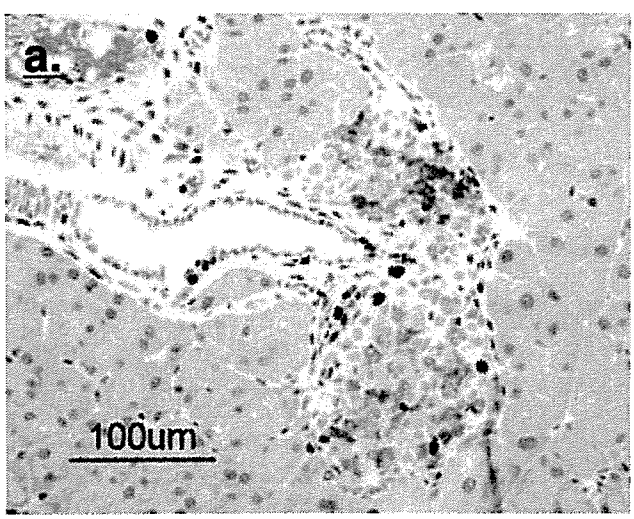

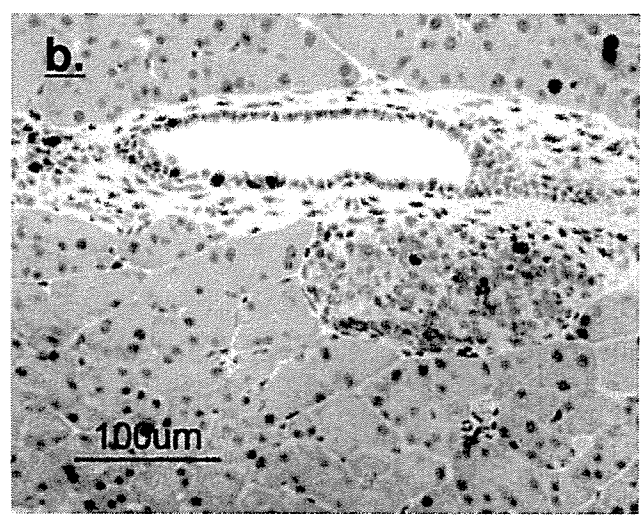

Hasegawa, et al. Figure 4

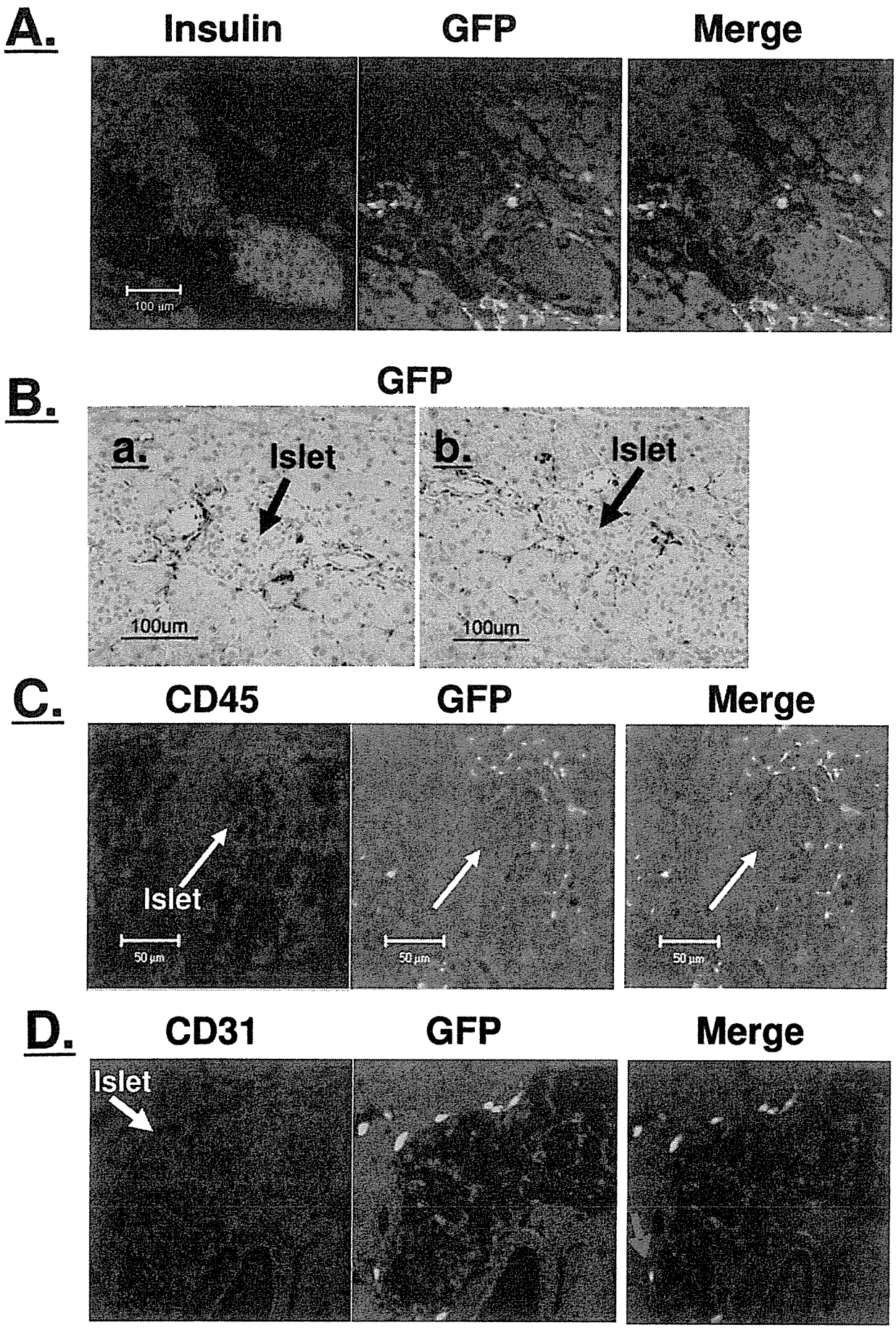

Hasegawa, et al. Figure 5

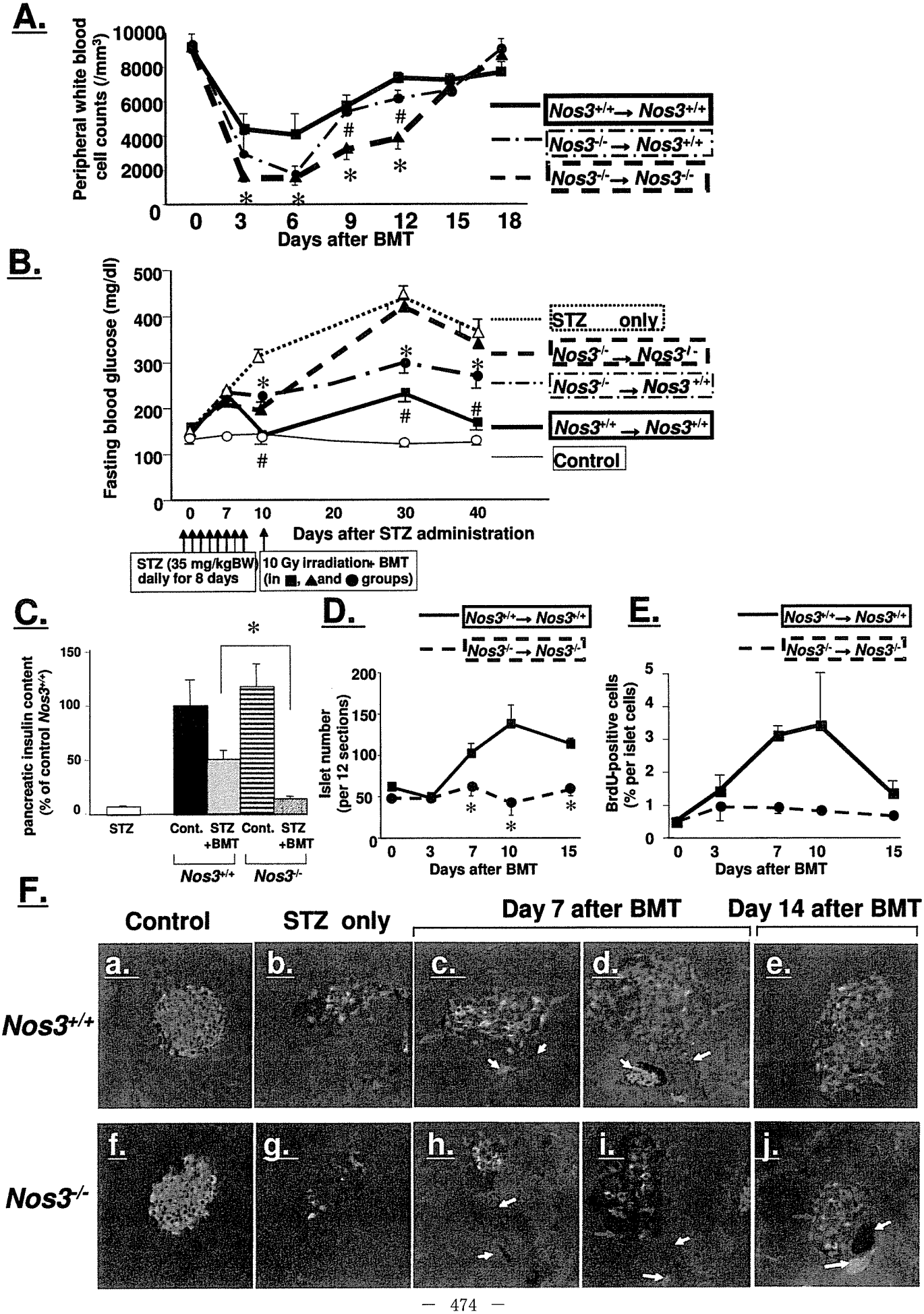

ELSEVIER

Atherosclerosis xxx (2006) xxx–xxx

ATHEROSCLEROSIS

www.elsevier.com/locate/atherosclerosis

A novel method for evaluating human carotid artery elasticity: Possible detection of early stage atherosclerosis in subjects with type 2 diabetes

Hisashi Okimoto[a,1], Yasushi Ishigaki[a,1], Yoshihiro Koiwa[b], Yoshinori Hinokio[a], Takehide Ogihara[c], Susumu Suzuki[a], Hideki Katagiri[c,f], Takayoshi Ohkubo[d,f], Hideyuki Hasegawa[e], Hiroshi Kanai[e], Yoshitomo Oka[a,g,*]

[a] *Division of Molecular Metabolism and Diabetes, Tohoku University Graduate School of Medicine, Japan*
[b] *Division of Cardiovascular Medicine, Tohoku University Graduate School of Medicine, Japan*
[c] *Division of Advanced Therapeutics for Metabolic Diseases, Tohoku University Graduate School of Medicine, Japan*
[d] *Department of Planning for Drug Development and Clinical Evaluation, Tohoku University Graduate School of Pharmaceutical Science and Medicine, Japan*
[e] *Department of Electrical Engineering, Tohoku University Graduate School of Engineering, Japan*
[f] *The 21st Century COE Programs, Comprehensive Research and Education Center for Planning of Drug Development and Clinical Evaluation, Japan*
[g] *The 21st Century COE Programs, Center for Innovative Therapeutic Development towards the Conquest of Signal Transduction Diseases, Tohoku University, Sendai, Japan*

Received 29 March 2006; received in revised form 5 September 2006; accepted 12 November 2006

Abstract

We recently developed a novel method for evaluating the elasticity of arterial walls, the phased tracking method. Herein, we evaluated atherosclerosis of the carotid artery with this method in 242 individuals with type 2 diabetes. In multiple regression analysis of subject status, age, systolic blood pressure and hyperlipidemia were found to be independently associated with carotid artery elasticity values. We also measured currently established values for atherosclerosis, carotid artery IMT and baPWV, in these subjects. Carotid artery elasticity correlated with max IMT ($r=0.291$, $p<0.01$), plaque score (PS) ($r=0.220$, $p<0.01$) and baPWV ($r=0.345$, $p<0.01$). Elasticity, max IMT and plaque score, all correlated with the number of risk factors for atherosclerosis, i.e. hypertension, hyperlipidemia and smoking, in addition to diabetes, consistent with the view that these values reflect atherosclerosis. Importantly, however, in subjects with IMT <1.1 mm, who are classified as not having atherosclerosis as defined by IMT criteria, only carotid artery elasticity correlated with the number of risk factors ($p<0.05$). These results suggest that (1) the measured carotid artery elasticity values reflect atherosclerosis and (2) our novel method has potential for detecting atherosclerosis in its early stage.

Keywords: Human carotid artery elasticity; Atherosclerosis; Diabetes

1. Introduction

Individuals with type 2 diabetes are at very high risk for atherosclerosis [1]. Although many methods have been developed for detecting atherosclerosis, those currently available are mainly for detecting established atherosclerosis. Therefore, the disease process is well-advanced at the time of diagnosis. To reduce future cardiovascular complications in subjects with atherogenic disorders such as type 2 diabetes

* Corresponding author at: Division of Molecular Metabolism and Diabetes, Tohoku University Graduate School of Medicine, 2-1 Seiryo-machi, Aoba-ku, Sendai 980-8575, Japan. Tel.: +81 22 717 7611; fax: +81 22 717 7611.
E-mail address: oka-y@mail.tains.tohoku.ac.jp (Y. Oka).
[1] These authors contributed equally to this work.

0021-9150/$ – see front matter © 2006 Elsevier Ireland Ltd. All rights reserved.
doi:10.1016/j.atherosclerosis.2006.11.020

Please cite this article in press as: Okimoto H, et al., A novel method for evaluating human carotid artery elasticity: Possible detection of early stage atherosclerosis in subjects with type 2 diabetes, Atherosclerosis (2006), doi:10.1016/j.atherosclerosis.2006.11.020

mellitus, detection of early stage atherosclerosis is urgently needed.

Carotid intima-media thickness (IMT) is a well-established surrogate marker for cardiovascular risk [2]. Measuring IMT with ultrasonography is non-invasive and relatively simple [3,4], and IMT is now commonly employed as an endpoint marker in clinical trials. Carotid IMT correlates with cardiovascular risk factors and indeed predicts macrovascular events such as myocardial infarction [5] and stroke [6]. Carotid IMT is greater in subjects with diabetes, both type 1 [7] and type 2 [8,9], than in non-diabetic subjects of the same age. When analyzed in diabetic patients, IMT correlates with glycemic control and the duration of diabetes. Interventions, such as blood glucose lowering [10], lipid lowering [11], ACE inhibition [12] and anti-platelet treatment [13], have been demonstrated to suppress IMT progression. However, it has also been reported that IMT is not affected by either therapeutic interventions [14] or glycemic control [15]. These conflicting results might be attributable to a very small change in IMT, a 0.1 mm increase per decade in normal subjects. Such a small change may mask actual change due to inter-assay variations in IMT measurement. Most importantly, it is not possible to make a diagnosis of atherosclerosis until the appearance of arterial wall thickening.

We recently developed a novel non-invasive method for evaluating the movement of multiple sites in cardiac and arterial walls (3.616 measurement sites/9.0 mm × 6.4 mm) during a single heartbeat [16,17]. This innovative phased tracking method enables us to evaluate regional characteristics; the softer the site, the more easily it deforms during one heartbeat. This reflects regional elasticity. This method has already been applied to the in vivo detection of regional changes in cardiac and arterial walls [18–20], and the interventricular septum [21]. Evaluation of plaque vulnerability has also been attempted [16]. It is theoretically possible to detect qualitative changes in the carotid arterial wall with this method. We therefore tested the possibility of being able to detect atherosclerosis in the early stage.

Herein, we show that carotid artery elasticity, as measured in Japanese subjects with type 2 diabetes, correlates well with results obtained with currently established methods for evaluating atherosclerosis. Most importantly, elasticity correlates with the number of risk factors for atherosclerosis in those with IMT <1.1 mm, who are classified as not having atherosclerosis as defined by IMT criteria [22,23]. These results strongly suggest that it is possible to detect early stage atherosclerosis with this novel method.

2. Methods

2.1. Study subjects

The study subjects were recruited from among patients followed at the diabetes clinic at Tohoku University Hospital. Patients with type 1 diabetes, renal failure (serum creatinine >2.0 mg/dl), severe heart failure (NYHA functional class 2–4), atrial fibrillation and peripheral arterial disease were excluded from the study. All participants analyzed were Japanese type 2 diabetes patients ($n = 242$) who met the WHO criteria for diabetes mellitus. The study protocol was approved by the Tohoku University Institutional Review Board. Informed consent was obtained from each patient. Subjects characteristics are shown in Table 1.

Table 1
Subject characteristics

Number	242
Age (years)	62.1 ± 12.4
Male (%)	54.1
Body weight (kg)	62.2 ± 13.6
BMI (kg/m^2)	24.2 ± 4.2
Duration of diabetes (years)	12.0 ± 9.70
Fasting blood glucose (mg/dl)	141 ± 32.1
HbA1c (%)	7.08 ± 1.33
Systolic blood pressure (mmHg)	130 ± 18.3
Diastolic blood pressure (mmHg)	75.8 ± 11.1
Total cholesterol (mg/dl)	191 ± 38.4
HDL cholesterol (mg/dl)	51.2 ± 14.6
LDL cholesterol (mg/dl)	115 ± 31.9
Triglyceride (mg/dl)	127 ± 94.1
Uric acid (mg/dl)	5.09 ± 1.37
High-sensitive CRP (mg/dl)	0.18 ± 0.23
Diabetic retinopathy (%)	30.2
Microalbumiuria or proteinuria (%)	38.8
Diabetic neuropathy (%)	46.4
Diet:OHA:insulin (%)	20.0:37.8:42.2
Hyperlipidemia (%)	37.2
Hypertension (%)	39.3
Current smoker (%)	30.6
BMI >25 (%)	38.0

Data are presented as means ± S.D.

We used the following criteria for atherogenic risk factors. Hyperlipidemia was defined as total cholesterol ≥5.7 mmol/dl (220 mg/dl) and/or triglyceride ≥1.7 mmol/l (150 mg/dl), based on the definition proposed by the Japan Atherosclerosis Society in 2002, or taking antihyperlipidemic drugs. The subjects whose systolic BP ≥140 mmHg and/or diastolic BP ≥90 mmHg (The Japanese Society of Hypertension guidelines in 2004) or who were taking antihypertensive drugs were defined as having hypertension. The subjects who currently smoked were classified as current smokers.

2.2. Measurement of ABI and baPWV

Ankle brachial pressure index (ABI) and brachial ankle pulse wave velocity (baPWV) were measured using an automatic waveform analyzer (BP-203RPE; Colin Co., Komaki, Japan) after a 5 min rest. This device was designed to simultaneously measure blood pressure levels in both arms (brachial arteries) and ankles (posterior tibial arteries), and to then calculate the ankle systolic BP/brachial systolic BP. Pulse waves were recorded on the right brachial artery and both posterior tibial arteries. The average baPWV was calculated by divid-

Please cite this article in press as: Okimoto H, et al., A novel method for evaluating human carotid artery elasticity: Possible detection of early stage atherosclerosis in subjects with type 2 diabetes, Atherosclerosis (2006), doi:10.1016/j.atherosclerosis.2006.11.020

ing the arm–ankle distance by the pulse wave transmission time between these points.

2.3. Measurement of carotid artery intima-media thickness

Intima-media thickness of the carotid arteries was measured using ultrasound diagnostic equipment (EUB-450, Hitachi Medico, Tokyo, Japan) with an electrical linear transducer (mid-frequency of 7.5 MHz). The common carotid artery (CCA), carotid bulb and portions of the internal and external carotid arteries on both sides were scanned with the subject in the supine position. The scan encompasses the region between 30 mm proximal to the beginning of the dilation of the bifurcation bulb and 15 mm distal to the CCA flow divider. We defined the max IMT as the thickest IMT in the scanned regions [24] and a max IMT <1.1 mm was considered normal. We defined a plaque, a focal IMT thickening, as an area with IMT $\geq$1.1 mm and calculated the plaque score (PS) by totaling the maximal thickness values of all plaques in the scanned area [25]. The scans were performed by a trained sonographer and the scanning period averaged 20 min in each patient.

2.4. Measurement of arterial wall elasticity

Real-time measurement of regional elasticity in the carotid artery wall was achieved based on a previously described method [20] with ultrasound diagnostic equipment (prototype system by Panasonic). With this system, an ultrasound beam is used for sequential scanning at 32 positions with a linear type 7.5 MHz probe. Multiple points were preset from the luminal surface to the adventitia along each beam with constant intervals of 320 μm, and multiple layers were defined as being between two neighboring points. Then, the displacement of each point preset along each beam was obtained by applying the phased tracking method to the received echo. Minute changes in the thickness of each layer were determined by subtracting displacements of two neighboring points. The elasticity of each layer was obtained from the thickness change and the blood pressure measured at the upper arm. Since the reflected ultrasound was resampled at an interval of 107 ns (=80 μm along the depth direction) after quadrature demodulation, we further divided each layer with a thickness of 320 μm into four points, shifted the initial depth of each layer by one-fourth of 320 μm, and applied the above procedure to each depth. Thus, the elasticity was obtained at intervals of 80 μm in the depth direction and 200 μm in the axial direction of the artery. A cross-sectional image and the process of elasticity measurement are schematically depicted in Fig. 1.

2.5. Statistical analysis

Variables were compared using Pearson's regression analysis and Student's *t*-test as appropriate. Then, a multiple linear regression analysis was performed to evaluate the independent parameters that were significantly related to arterial elasticity. The relationships between number of risk factors and the values of atherosclerosis markers were examined by analysis of covariance (ANCOVA), adjusted with age as a covariate. A p value less than 0.05 was accepted as indicating statistical significance. All statistical analyses were performed using the Statistical Package for the Social Sciences Version 13.0 (SPSS Japan Inc., Tokyo, Japan).

3. Results

We assessed the associations of carotid artery elasticity with subject characteristics (Table 2). Elasticity correlated

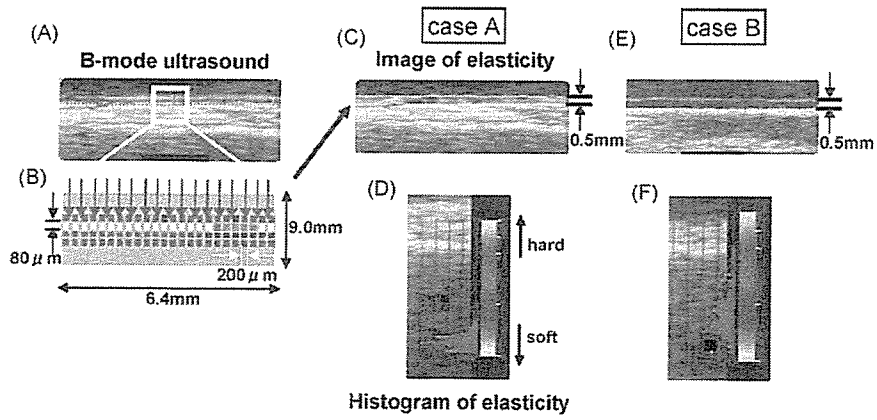

Fig. 1. The intima–media complex was visualized by conventional B-mode scanning (A), and minute thickness changes in the layers at each depth (113 depths × 32 beams per 9 mm × 6.4 mm scanned area) during one heart beat were then recorded by the phased tracking method (B). Thickness changes in each layer represent deformity, a reflection of elasticity. This elasticity is displayed as a 2D cross-sectional color image on B-mode scanning, and the image is updated at every heartbeat (C). The elasticity distribution is shown as a histogram (D). Representative results obtained from a normal subject, case A (male, age 40), are shown. Case B (male, age 45), in marked contrast, suffered from type 2 diabetes, hyperlipidemia and an old cerebral infarction, but had an IMT of only 0.5 mm, the same thickness as that of case A. The elasticity (E) was, however, extremely different from that of case A, as shown in the histogram (F).

Please cite this article in press as: Okimoto H, et al., A novel method for evaluating human carotid artery elasticity: Possible detection of early stage atherosclerosis in subjects with type 2 diabetes, Atherosclerosis (2006), doi:10.1016/j.atherosclerosis.2006.11.020

Table 2
Associations between arterial elasticity and subject characteristics

Variables	r-Value	p-Value
Age	0.34	<0.01
Duration of diabetes	0.136	<0.05
Fasting blood glucose	−0.012	0.86
HbA1c	−0.003	0.97
Total cholesterol	0.103	0.10
HDL cholesterol	0.066	0.31
LDL cholesterol	0.089	0.17
Triglyceride	−0.064	0.32
Systolic blood pressure	0.443	<0.01
Diastolic blood pressure	0.147	<0.05
Uric acid	−0.03	0.65
High-sensitive CRP	0.037	0.56

Table 3
Mean arterial elasticity values in the presence and absence of cardiovascular risk factors

Variables	Elasticity (kPa)		p
	−	+	
Male	51.6 ± 12.6	51.0 ± 14.5	0.99
Hyperlipidemia	49.8 ± 12.3	54.7 ± 13.7	<0.01
Hypertension	49.6 ± 13.3	54.8 ± 13.6	<0.01
Current smoker	51.6 ± 13.3	51.8 ± 14.5	0.88
BMI >25	51.6 ± 13.7	51.6 ± 13.5	0.99
Diabetic retinopathy	52.3 ± 13.7	50.9 ± 14.1	0.67
Diabetic nephropathy	50.5 ± 13.6	53.9 ± 13.6	0.06
Diabetic neuropathy	50.8 ± 12.9	51.4 ± 14.4	0.65

Data are presented as means ± S.D.

Table 4
Multivariate adjustment for parameters related to arterial elasticity

Variables	Coefficient (β)	95% CI	p-Value
Age (years)	0.28	0.18–0.43	<0.01
Duration of diabetes (years)	−0.02	−0.18–0.14	0.77
Systolic blood pressure (mmHg)	0.39	0.21–0.38	<0.01
Hyperlipidemia	0.11	0.08–6.24	<0.05

with age ($r=0.340$, $p<0.01$), duration of diabetes ($r=0.136$, $p<0.05$) and blood pressure, both systolic ($r=0.430$, $p<0.01$) and diastolic ($r=0.147$, $p<0.05$).

We then examined whether or not cardiovascular risk factors affect arterial elasticity values (Table 3). Hyperlipidemic subjects had significantly higher arterial elasticity values than those with normal lipid profiles. Similarly, subjects with hypertension had higher values. However, arterial elasticity values did not depend on other risk factors, such as sex, obesity, smoking and diabetic complications.

To elucidate the independent variables affecting arterial elasticity, we performed multiple linear regression analysis with parameters related to elasticity. We employed four clinical parameters, age, duration of diabetes, systolic blood pressure and hyperlipidemia, based on the results shown in Tables 2 and 3. We found age, systolic blood pressure and hyperlipidemia to be independently associated with elasticity values (Table 4).

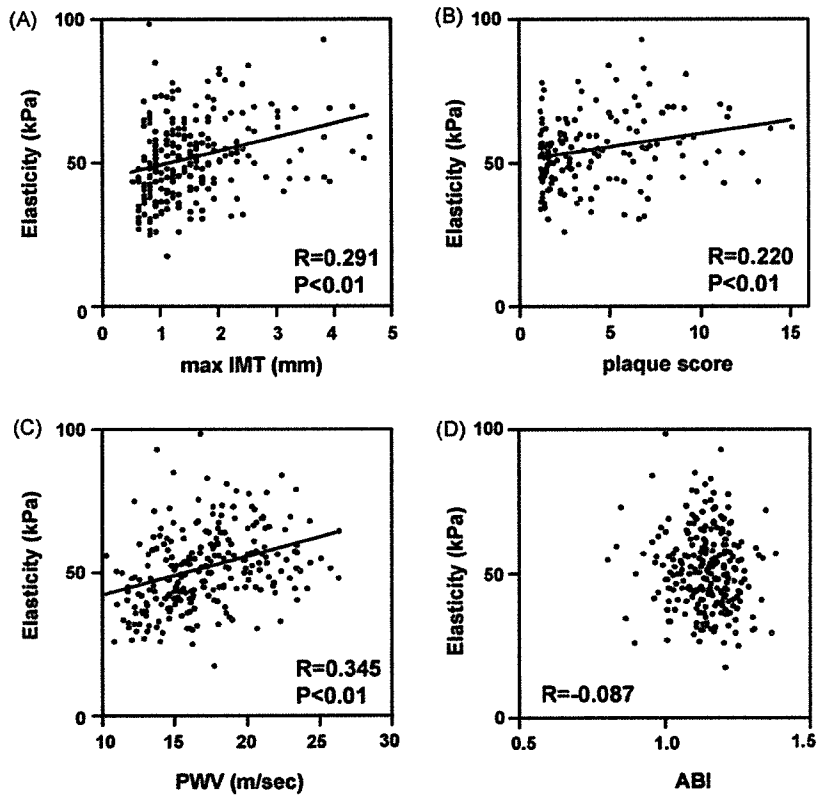

Fig. 2. Correlations between arterial elasticity values and max IMT (A), plaque score (B), baPWV (C) and ABI (D).

Please cite this article in press as: Okimoto H, et al., A novel method for evaluating human carotid artery elasticity: Possible detection of early stage atherosclerosis in subjects with type 2 diabetes, Atherosclerosis (2006), doi:10.1016/j.atherosclerosis.2006.11.020